Part II

Diluted Magnetic Semiconductors

First-Principles Study of the Magnetism of Diluted Magnetic Semiconductors

L.M. Sandratskii and P. Bruno

Max-Planck Institut für Mikrostrukturphysik, Weinberg 2, D-06120 Halle, Germany,
lsandr@mpi-halle.de
bruno@mpi-halle.de

Abstract. We report the density-functional-theory calculations of the exchange interactions and Curie temperature for a series of III-V and II-VI diluted magnetic semiconductors. We focus the discussion on the role of the holes in the establishing the ferromagnetic order in various systems. We suggest a method of the quantitative characterization of the properties of the holes. It is shown that there are two conflicting properties of the holes – delocalization from impurity and p–d interaction – whose combination determines the hole influence on the Curie temperature. We demonstrate that Hubbard U increases delocalization of the holes and decreases the strength of p-d interaction. Depending on the system these competing trends can lead to both increase and decrease of the Curie temperature. We show that high value of the Curie temperature for low impurity concentration is possible only in the case of substantial admixture of the impurity 3d states to hole states.

1 Introduction

An important current problem towards practical use of the spin-transport in semiconductor devices is the design of the materials that make possible the injection of spin-polarized electrons into a semiconductor at room temperature. One of the promising classes of materials are diluted magnetic semiconductors (DMS). A strong interest to these systems was attracted by the observation [1] in $Ga_{0.947}Mn_{0.053}As$ of the ferromagnetism with the Curie temperature (T_C) as high as 110 K. To design materials with Curie temperature higher than room temperature the knowledge of physical mechanisms governing the exchange interactions in DMS is of primary importance.

Despite much work devoted to the study of DMS the situation is still controversial from both experimental and theoretical points of view. The complexity of the experimental situation is well illustrated by the case of (GaMn)N. After the theoretical prediction of high-temperature ferromagnetism in (GaMn)N by Dietl et al. [2] this system was produced and investigated in many experimental groups. The spectrum of the magnetic states reported ranges from paramagnetic and spin-glass states to the ferromagnetism with extremely high T_C of 940 K [3, 4, 5]. A further proof of the complexity of the magnetism of (GaMn)N was given by recent magnetic circular dichroism

L.M. Sandratskii and P. Bruno: *First-Principles Study of the Magnetism of Diluted Magnetic Semiconductors*, Lect. Notes Phys. **678**, 113–130 (2005)
www.springerlink.com
© Springer-Verlag Berlin Heidelberg 2005

measurements by Ando [6]. The measurements were performed on a high-T_C sample and led Ando to the conclusion that the (GaMn)N phase in this sample is paramagnetic. The ferromagnetism of the sample was claimed to come from an unidentified phase. On the other hand, in a recent preprint by Giraud et al. [7] a high temperature ferromagnetism was detected in samples with a low Mn concentration of about 2%. The authors rule out the presence of precipitates in the system and argue that the room temperature ferromagnetism is an intrinsic property of (GaMn)N.

Likewise, the theoretical situation is not uniform. The theoretical works on the ferromagnetism in the DMS systems can be separated into two groups. The first group models the problem with an effective Hamiltonian containing experimentally determined parameters. This part of the studies was recently reviewed in [8, 9, 10] Different assumptions concerning the energy position and the role of the 3d sates of the magnetic impurities are formulated. Different types of the exchange interactions – potential exchange, kinetic exchange, superexchange, double exchange, RKKY exchange, Blombergen-Rowland exchange and others – are invoked to describe the properties of the system. Most of the model-Hamiltonian studies agree with each other in that the presence of holes plays important role in ferromagnetism of DMS.

The second group of theoretical studies is based on the parameter-free calculations within the density functional theory (DFT) (see, e.g., reviews [11, 12] and more recent work [13, 14, 15, 16, 17]). The DFT calculations intend to treat realistic systems in their detailed complexity. In particular, every electron state is involved in effective exchange interaction with all other electron states [18]. Therefore different types of exchange interactions intermix and influence each other. The complexity of the DFT picture reflects the complexity of the real systems. To gain deeper qualitative understanding of the magnetism of the system it is, however, very useful to relate the DFT results to the results of the model-Hamiltonian treatments attempting to single out the leading exchange mechanisms responsible for the establishing of the long range magnetic order.

In this paper we report DFT calculations for a number of III-V and II-VI DMS. To develop a general platform for discussion of various systems we focus on the role of the holes in the magnetism of DMS. First, we reexamine the importance of the holes for establishing the long-range ferromagnetic order. Then we discuss the properties of the holes that are relevant for the ferromagnetic ordering and consider quantitative characterization of these properties. We investigate the influence of the on-site Coulomb interaction on the properties of the holes. We study the connection between the combination of the hole features, on the one hand, and the effective exchange interactions between the magnetic impurities and the Curie temperature, on the other hand.

The main body of calculations is performed within the local density approximation (LDA) to the DFT. An important issue in the physics of DMS

is the role of the Coulomb correlations of the 3d electrons. The so-called LDA+U method introduces explicitly the on-site Coulomb interaction (Hubbard U) and leads to a better description of many systems with strong Coulomb correlations [19]. However, the superiority of the LDA+U method is not universal. For numerous systems with 3d atoms the LDA gives better agreement with experiment.

In the paper, we report both LDA and LDA+U calculations for a number of DMS. The influence of Hubbard U on various electron properties of the systems is analyzed. Where possible the results of both calculations are compared with experiment to establish which of two approaches provides better description of the DMS studied.

2 Calculational Technique

The calculational scheme is discussed in [13, 14, 20] to which the reader is referred for more details. The scheme is based on DFT calculations for supercells of semiconductor crystals with one cation atom replaced by a Mn atom. The size of the supercell determines the Mn concentration. Most of the calculations are performed for the zinc-blende crystal structure of the semiconductor matrix.

To calculate the interatomic exchange interactions we use the frozen-magnon technique and map the results of calculation of the total energy of the helical magnetic configurations

$$\mathbf{e}_n = (\cos(\mathbf{q}\cdot\mathbf{R}_n)\sin\theta,\ \sin(\mathbf{q}\cdot\mathbf{R}_n)\sin\theta,\ \cos\theta) \tag{1}$$

onto a classical Heisenberg Hamiltonian

$$H_{eff} = -\sum_{i\neq j} J_{ij}\mathbf{e}_i\cdot\mathbf{e}_j \tag{2}$$

where J_{ij} is an exchange interaction between two Mn sites (i,j) and $\mathbf{e}_i$ is the unit vector pointing in the direction of the magnetic moment at site i, $\mathbf{R}_n$ are the lattice vectors, $\mathbf{q}$ is the wave vector of the helix, polar angle θ gives the deviation of the moments from the z axis.

A deviation of the atomic moments from the parallel directions causes a change of the atomic exchange-correlation potentials [21] which leads to a perturbation of the electron states. The value of the perturbation of a given state depends on other states of the system, both occupied and empty, since these states enter the secular matrix of the problem.

Within the Heisenberg model (2) the energy of frozen-magnon configurations can be represented in the form

$$E(\theta,\mathbf{q}) = E_0(\theta) - \sin^2\theta J(\mathbf{q}) \tag{3}$$

where E_0 does not depend on $\mathbf{q}$ and $J(\mathbf{q})$ is the Fourier transform of the parameters of the exchange interaction between pairs of Mn atoms:

$$J(\mathbf{q}) = \sum_{j \neq 0} J_{0j} \, \exp(i\mathbf{q} \cdot \mathbf{R_{0j}}) \, . \tag{4}$$

Performing back Fourier transformation we obtain the parameters of the exchange interaction between Mn atoms:

$$J_{0j} = \frac{1}{N} \sum_{\mathbf{q}} \exp(-i\mathbf{q} \cdot \mathbf{R_{0j}}) J(\mathbf{q}) \, . \tag{5}$$

The Curie temperature is estimated in the mean-field (MF) approximation

$$k_B T_C^{MF} = \frac{2}{3} \sum_{j \neq 0} J_{0j} \tag{6}$$

We use a rigid band approach to calculate the variation of exchange parameters and Curie temperature with respect to electron occupation. We assume that the electron structure calculated for a DMS with a given concentration of the 3d impurity is basically preserved in the presence of defects. The main difference is in the occupation of the bands and, respectively, in the position of the Fermi level.

In the LDA+U calculations we use $U = 0.3$ Ry that corresponds to the value determined experimentally [22].

3 Single Band in the Frozen-Magnon Field

Pursuing the aim to place the role of the holes in the focus on the discussion we begin with the consideration of a simple model of one spin-degenerate band in a helical exchange field. Such a field corresponds to the exchange field originating from the frozen magnon. We discuss the role of electrons in almost empty band and holes in almost filled band in establishing the ferromagnetic order.

The frozen magnons are defined by (1). The exchange field acting on the band is taken in the form $\mathbf{b}_n = \Delta \, \mathbf{e}_n$ where Δ is the amplitude of the field.

The secular matrix of a tight-binding model takes in this case the form

$$\begin{pmatrix} \cos^2(\frac{\theta}{2}) H_- + \sin^2(\frac{\theta}{2}) H_+ - \frac{\Delta}{2} & -\frac{1}{2} \sin\theta (H_- - H_+) \\ -\frac{1}{2} \sin\theta (H_- - H_+) & \sin^2(\frac{\theta}{2}) H_- + \cos^2(\frac{\theta}{2}) H_+ + \frac{\Delta}{2} \end{pmatrix} \tag{7}$$

where $H_- = H(\mathbf{k} - \frac{1}{2}\mathbf{q})$, $H_+ = H(\mathbf{k} + \frac{1}{2}\mathbf{q})$, and $H(\mathbf{k})$ describes spin-degenerate bands of a non-magnetic crystal.

The eigenvalues of the matrix (7) have the form

$$\varepsilon_{\pm}(\mathbf{k}) = \frac{1}{2}(H_- + H_+) \tag{8}$$
$$\pm(\frac{1}{4}(H_- - H_+)^2 - \frac{1}{2}\Delta\cos\theta(H_- - H_+) + \frac{1}{4}\Delta^2)^{\frac{1}{2}}$$

and are illustrated in Fig. 1.

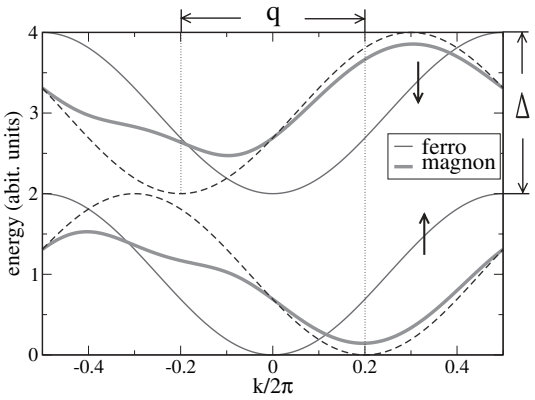

Fig. 1. The energy bands (*thick solid line*) of the spiral structure with $\mathbf{q} = 0.8\pi$, $\Delta = 2$, and $\theta = 45°$. $H(\mathbf{k}) = 1 - \cos(k)$. The lattice parameter is assumed to be unity. The *thin solid lines* show the bands of a ferromagnetic configuration. The broken lines give the ferromagnetic bands shifted in the reciprocal space according to the given $\mathbf{q}$

For completely filled bands the total energy

$$E_b = \frac{1}{\Omega_{BZ}}\int_{\mathrm{BZ}} d\mathbf{k}[(\varepsilon_-(\mathbf{k}) + \varepsilon_+(\mathbf{k})] = \frac{2}{\Omega_{BZ}}\int_{\mathrm{BZ}} d\mathbf{k}H(\mathbf{k}) \tag{9}$$

does not depend on magnetic configuration. [Ω_{BZ} is the volume of the Brillouin zone (BZ)]. This means that the kinetic exchange taken into account by (7) does not contribute into effective intersite exchange interaction in the case of completely filled bands.

For almost empty and almost filled bands the minimum of the total energy always corresponds to the ferromagnetic configuration. For a detailed proof of this statement the reader is referred to [14]. Figure 1 illustrates that under the influence of the frozen magnon the bands become narrower: The minimal electron energy of the ferromagnet is lower than the minimal electron energy of the spiral and the maximal electron energy of the ferromagnet is higher than the maximal energy of the spiral. In combination with (9) this is sufficient to prove that small number of electrons or small number of holes lead to the ferromagnetic ground state.

Thus within the model of a single spin-degenerated band in a frozen-magnon exchange field the presence of holes makes the ferromagnetic structure favorable. In the following sections we show that the importance of the holes for establishing ferromagnetic order is preserved in the full–scale DFT calculations.

4 Results for (GaMn)As,(GaCr)As,(GaFe)As

Next we consider calculations for three III-V DMS: (GaMn)As, (GaMn)As and (GaFe)As. Figure 2 presents the DOS of the systems for the impurity concentration of 3.125%. For comparison the GaAs DOS is shown. In the case of (GaMn)As the replacement of one Ga atom in the supercell of GaAs by a Mn atom does not change the number of spin-down states in the valence band. In the spin-up chanel there are, however, five additional energy bands which are related to the Mn 3d states. Since there are five extra energy bands and only four extra valence electrons (the atomic configurations of Ga and Mn are $4s^2 4p^1$ and $3d^5 4s^2$) the valence band is not filled and there appear unoccupied (hole) states at the top of the valence band. There is exactly one hole per Mn atom.

In (GaCr)As, the Cr 3d states assume a higher energy position relative to the semiconductor-matrix states than the Mn 3d states in (GaMn)As. As a result, the spin-up impurity band is separated from the valence band and lies in the semiconducting gap of GaAs. This impurity band contains three energy bands. Since Cr has one electron less than Mn, only one third of the impurity band is occupied: the occupied part contains one electron per Cr atom and there is place for further two electrons.

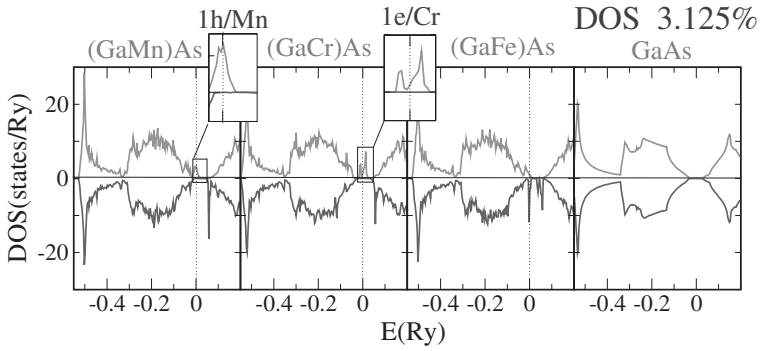

Fig. 2. The spin-resolved DOS for (GaMn)As, (GaCr)As, (GaFe)As. For comparison the DOS of GaAs is shown. The concentration of Mn is 3.125%. *Upper part* of the graph shows spin-up DOS. The inserts zoom the important energy regions about the Fermi level. In (GaMn)As there is one hole per Mn atom. In (GaCr)As there is one electron per Cr atom in the impurity band

In (GaFe)As the number of valence electrons is by one larger than in (GaMn)As. Simultaneously, the Fe 3d states assume lower energy position with respect to the semiconductor matrix than Mn 3d states. As a result, the spin-down Fe 3d states become partly occupied. There are carriers in both spin-channels.

In Fig. 3 we show calculated mean-field Curie temperatures. For (GaMn)As and (GaCr)As we obtained rather similar results at least for realistic impurity concentrations below 15%. In the case of (GaFe)As there is a clear trend to antiferromagnetism.

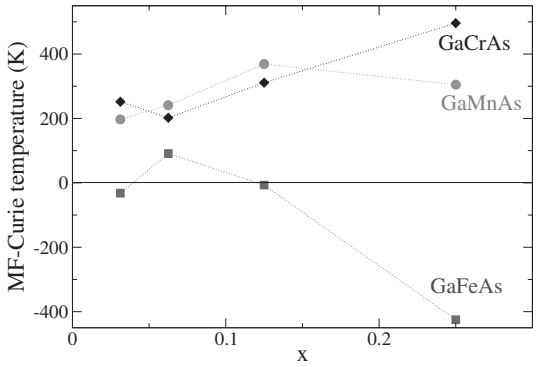

Fig. 3. The mean-field Curie temperature. The negative values of the Curie temperature reveal the prevailing antiferromagnetic exchange interactions and instability of the ferromagnetic state

(GaCr)As and (GaFe)As are not yet sufficiently studied experimentally. For (GaMn)As our result of high Curie temperature for low Mn concentrations is in good correlation with experiment. Our estimation of the Curie temperature is substantially higher than the early experimental value of 110 K for $Ga_{0.947}Mn_{0.053}As$. However, later measurements [23] on samples with less uncontrolled defects gave higher Curie temperature of 150 K that is closer to our estimation.

An important issue in DMS on the GaAs basis is the presence of donor defects, in particular As_{Ga} antisites, compensating part of the holes. Thus the number of holes per Mn atom is usually smaller than one. To study this effect we performed calculations for varied band occupation. An increase of band occupation leads to a decrease of the number of holes and vice versa. The results are shown in Fig. 4. In the case that all energy bands are either completely filled or empty [these are the point of $n = 1$ for (GaMn)As and the points $n = -1$ and $n = 2$ for (GaCr)As (Fig. 4)] the antiferromagnetic interatomic exchange interactions always prevail. This agrees with the picture of Anderson's antiferromagnetic superexchange. In (GaMn)As there is a clear trend to decreasing T_C for hole number less than the nominal value of one.

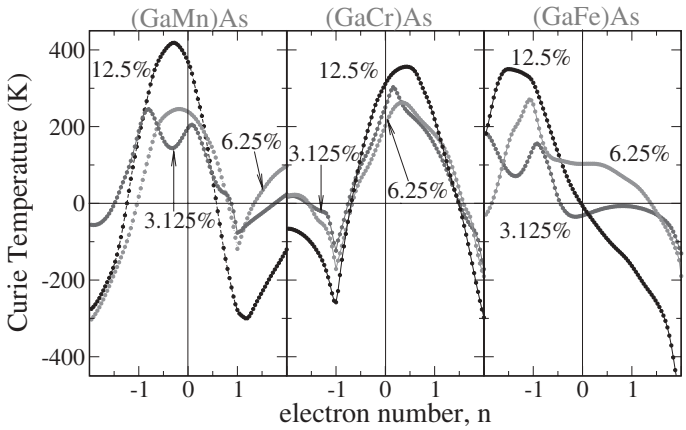

Fig. 4. The Curie temperature as a function of the electron number. n is the number of the excess electrons (or missing electrons for negative values) per magnetic impurity atom. The nominal electron number corresponds to $n = 0$. In all cases of completely filled electron bands (kinks on the curves) the prevailing exchange interactions are antiferromagnetic

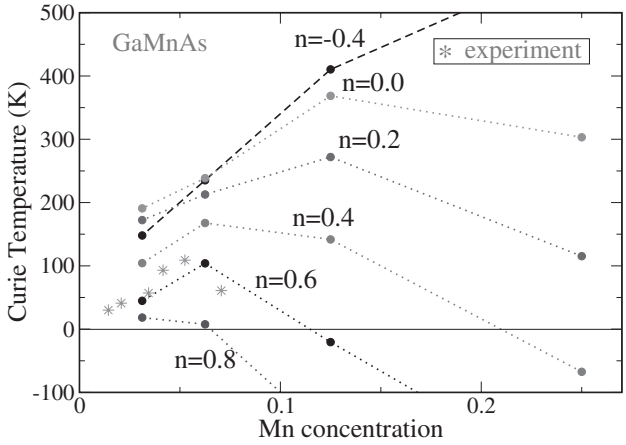

Fig. 5. The Curie temperature of (GaMn)As as a function of Mn concentration for different numbers of holes. The experimental values are taken from [24]

In Fig. 5 we show the Curie temperature as a function of Mn concentration for different numbers of holes per Mn atom. For the case of $n = 0.6$ (that is 0.4 hole per Mn atom) the calculated Curie temperatures are close to the experimental values.

In (GaCr)As the situation is different. Because of a decreased number of valence electrons the impurity band can accept two further electrons per Cr atom and is far from the full occupation. As a result the donor defects do not

exert in this case the strong influence obtained for (GaMn)As: One compensating electron makes (GaMn)As antiferromagnetic whereas the Curie temperature of (GaCr)As changes only weakly. On the other hand, the acceptor defects influence strongly the Curie temperature of (GaCr)As: a decreasing number of valence electrons below the nominal value marked by $n = 0$ in Fig. 4 leads to a fast decrease of the interatomic exchange parameters resulting in the change of the sign of the parameters and in the transition from ferromagnetic to antiferromagnetic exchange interactions. At $n = -1$ the impurity band becomes empty that corresponds to the strongest antiferromagnetic interactions (minimum of T_C in Fig. 4).

The result for (GaFe)As differ drastically from the results for both (GaMn)As and (GaCr)As. Here, already for nominal electron number ($n = 0$) the antiferromagnetic interactions become stronger than ferromagnetic. The reasons for this are a small number of the holes in the spin-up chanel and a very narrow impurity band in the spin-down chanel.

Summarizing, our calculations show that the partial occupation of the energy bands is essential for the formation of ferromagnetic order.

5 (ZnCr)Te

The calculational technique discussed above is universal and can be applied to both III-V and II-VI DMS. In this Section we discuss the study of the II-VI DMS (ZnCr)Te. A strong interest to this system is attracted by the recent experiment by Saito et al [25] who detected the ferromagnetism of $Zn_{0.8}Cr_{0.2}Te$ with the Curie temperature of 300 K, together with magneto-optical evidence in favor of an intrinsic (i.e., hole mediated) mechanism of ferromagnetism.

The cations in II-VI semiconductors have one additional valence electron compared to the cations in III-V systems. Therefore the replacement of a cation atom by a Mn atom is not expected to result in partially filled bands. The situation changes in the case of Cr doping since one Cr atom has one valence electron less than one Mn atom.

We performed calculations for $Zn_{0.75}Cr_{0.25}Te$ [26] and found a number of features similar to the properties of (GaMn)As. The calculated DOS is shown in Fig. 6. The system is half-metallic. There is exactly one hole per Cr atom in the spin-up valence band.

The calculated Curie temperature is shown in Fig. 7. The decreasing number of holes leads to a transition from ferromagnetic to antiferromagnetic exchange interactions. As expected, the doping with Mn does not result in partially filled bands. Correspondingly (ZnMn)Te is antiferromagnetic for nominal number of valence electrons. Remarkable that $T_C(n)$ curves for (ZnCr)Te and (ZnMn)Te are similar with the major difference consisting in the shift by one along the axis of band occupation. This result shows the validity of the rigid band model for qualitative considerations.

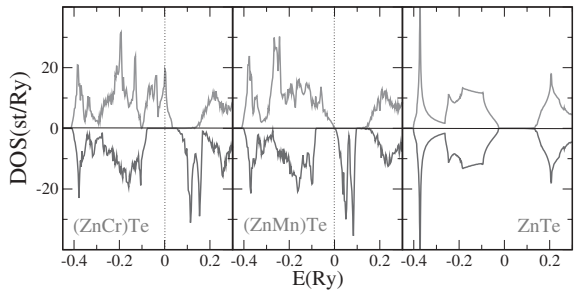

Fig. 6. The DOS of $Zn_{0.75}Cr_{0.25}Te$ and $Zn_{0.75}Mn_{0.25}Te$. For comparison the DOS of ZnTe is shown

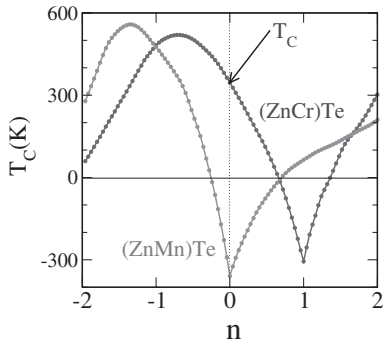

Fig. 7. The Curie temperature of (ZnCr)Te and (ZnMn)Te as a function of the electron number

6 Properties of the Holes and Magnetism

In previous sections we have shown the crucial role of the partially filled bands in the ferromagnetism of III-V and II-VI DMS. To gain a deeper insight in the mechanisms of the formation of ferromagnetism we take a closer look at the properties of the holes relevant to the establishing the long-range order. Two features of the holes are important: the delocalization from the impurity, on the one hand, and the interaction between the hole and the magnetic impurity (p–d interaction), on the other hand. Figure 8 illustrates schematically the necessity of both components. For comparison of different systems it is important to characterize the properties of the holes quantitatively. The numerical characterization of the hole delocalization is rather straightforward: The spatial distribution of the hole can easily be obtained within DFT calculations on the basis of the known wave functions of the electron states.

A quantitative characterization of the p–d interaction is less straightforward. In the mean-field approximation, the parameter $N\beta$ describes the spin-splitting of the semiconductor valence-band states

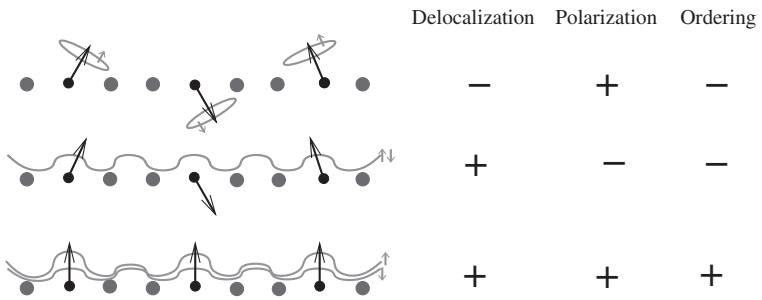

Fig. 8. Both delocalization of the holes and the exchange interaction hole-impurity are crucial for establishing ferromagnetic order. The upper line shows schematically the holes localized about the impurity atoms. The holes are strongly spin-polarized but do not mediate the exchange interaction between impurities. In the second line, the holes are not disturbed by the impurities and are completely delocalized. They, however, are not spin-polarized by the impurities and also cannot mediate the exchange interaction. The third line presents an intermediate situation: The hole states are disturbed by the impurities. They are, however, not completely localized about the impurity. Combination of the delocalization and spin-polarization allows to mediate exchange interaction between Mn atoms

$$\varepsilon_{\downarrow} - \varepsilon_{\uparrow} = N\beta \langle S \rangle x \tag{10}$$

which appears as a consequence of the interaction of these states with Mn 3d electrons. In (10), $\langle S \rangle$ is the average atomic spin moments of the magnetic impurities, x is the impurity concentration. However, the applicability of the mean-field approach is not self-evident and needs to be investigated.

The analysis of the experimental data shows that for II-VI DMS the value of $N\beta$ is well established [27]. For III-V systems the situation is different. For instance, the experimental estimations of $N\beta$ made for (GaMn)As on the basis of different experimental techniques vary strongly from large values of $|N\beta| = 3.3$ eV [24] and $N\beta = 2.5$ eV [28] to a much smaller value of $N\beta = -1.2$ eV [22]. (Negative $N\beta$ corresponds to antiparallel directions of the spins of the d and p states.) In Fig. 9 we present the calculated exchange splitting at the top of the valence band in (ZnMn)Se. For low Mn concentrations this system is paramagnetic up to very low temperatures. It shows, however, a giant Zeeman splitting in external magnetic field. The giant Zeeman splitting reveals strong p–d exchange interaction.

Two DFT approaches are used: LDA and LDA+U (Fig. 9). The LDA+U exchange splittings are well described by the mean-field formula (10) that assumes proportionality between the splitting and the Mn concentration. The coefficient proportionality gives the value of $N\beta = -1.3$ eV in very good agreement with experiment. On the other hand, the LDA results deviate strongly from the mean-field behavior. The LDA calculations does not give the proportionality between splitting and concentration. Correspondingly, the ratio between the splitting and the concentration varies with the

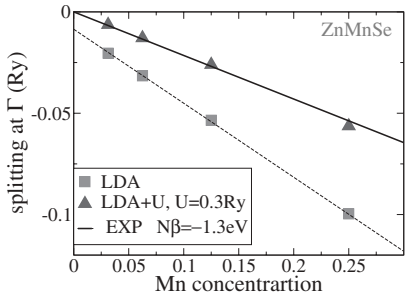

Fig. 9. The exchange splitting at at the top of the valence band (Γ point). Calculations are performed within LDA and LDA+U. The *solid line* corresponds to the experimental value of the $N\beta$ parameter [8]

concentration and has larger absolute value than the corresponding LDA+U estimation. The LDA results do not give good agreement with experimental value of $N\beta$ for (ZnMn)Se. They, however, remind us the experimental situation for (GaMn)As where some of the estimated values of $N\beta$ are larger than in the case of (ZnMn)Se and there is a strong variation of $N\beta$ from estimation to estimation.

To understand the origin of the difference between LDA and LDA+U results we compare in Fig. 10 the DOS of (ZnMn)Se calculated within both approaches. We obtain very strong difference between two DOS: Whereas the LDA DOS possesses substantial Mn 3d contribution at the top of the valence

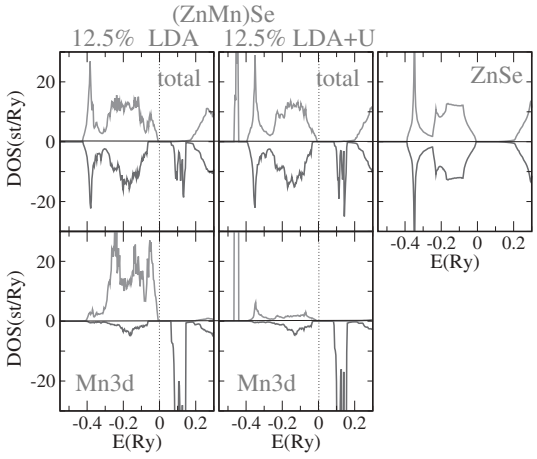

Fig. 10. The total and partial Mn 3d DOS of $Zn_{0.875}Mn_{0.125}Se$. For comparison the DOS of ZnSe is presented. In LDA+U calculation $U = 0.3$ Ry

band the account for Hubbard U results in a strong decrease of the Mn 3d contribution in this energy region. The failure of the mean-field treatment to describe the LDA splittings is directly related to the strong admixture of the Mn 3d states. Since the atomic Mn moment in (ZnMn)Se does not depend substantially on the Mn concentration the exchange splitting of the Mn 3d states cannot be described within a mean-field approximation.

Summarizing we formulate some conclusions: First, in the case of substantial admixture of the impurity 3d states to the states at the top of the valence band the mean-field approach to the characterization of the p–d interaction does not apply. Second, in the case of (ZnMn)Se the application of the LDA+U scheme leads to the shift of the Mn 3d spin-up states from the top of the valence band to lower energies making the mean-field approximation applicable. Third, for (ZnMn)Se the LDA+U gives better overall agreement with experiment than LDA [29].

7 Comparative Study of (GaMn)As and (GaMn)N

In this section we compare the magnetism of two prototype systems, (GaMn)As and (GaMn)N, focusing again on the properties of the holes. To circumvent the difficulty of the estimation of the $N\beta$ parameter we will characterize the strength of the p–d interaction by the value of the admixture of the 3d states to the hole. This quantity is difficult to measure but it is easily accessible theoretically. This section is based on the paper [30].

In Figs. 11,12, we present the DOS of (GaMn)As and (GaMn)N for $x = 12.5\%$. The main features of the DOS discussed below are valid also for other Mn concentrations.

We found that (GaMn)As and (GaMn)N differ strongly in both LDA and LDA+U calculations. In LDA, the spin-up impurity band of (GaMn)As merges with the valence band. On the other hand, in (GaMn)N the impurity band lies in the semiconducting gap. (We performed calculations for both zinc-blende and wurzite crystal structures of (GaMn)N. The main part of the results is qualitatively similar for both crystal structures.) For both systems the LDA calculations give large Mn 3d contribution into impurity band (Fig. 12).

In the LDA+U calculations, the impurity band of (GaMn)As disappears from the energy region at the top of the valence band. In contrast, (GaMn)N still possesses impurity band which lies now closer to the valence band. The Mn 3d contribution to the impurity band decreases compared with the LDA-DOS but is still large (Fig. 12).

Now we turn to the discussion of the properties of the holes. We again present the results for one Mn concentration. From Fig. 13 and Table 1 we see that for the calculations performed within the same calculational scheme the holes in (GaMn)N are much stronger localized about the Mn atom than

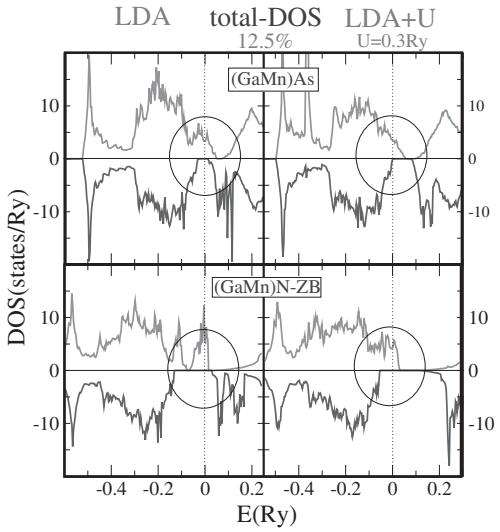

Fig. 11. The total DOS of $Ga_{0.875}Mn_{0.125}As$ and $Ga_{0.875}Mn_{0.125}N$ calculated within LDA and LDA+U approaches. The circles highlight the part of the DOS that is most important for the discussion

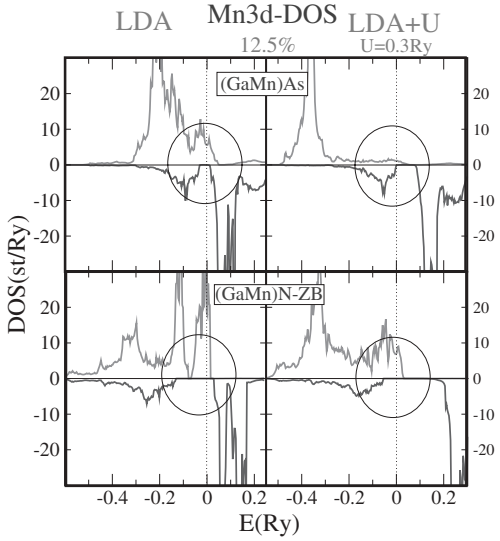

Fig. 12. The Mn 3d DOS of $Ga_{0.875}Mn_{0.125}As$ and $Ga_{0.875}Mn_{0.125}N$

in (GaMn)As. The Mn 3d contribution into the hole, and therefore the p–d interaction, is also stronger in (GaMn)N. Thus there are two competing trends in the properties of the holes. To predict the relation between the Curie temperatures of both systems a direct calculation of the Mn-Mn exchange

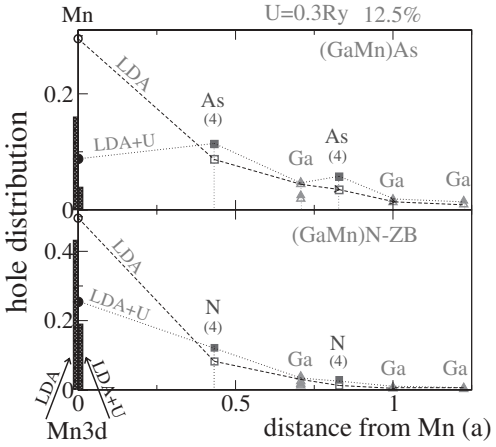

Fig. 13. Distribution of the hole in LDA and LDA+U calculations. Numbers in parentheses give the number of atoms in the coordination sphere. The hole part is given for one atom. The distance from Mn is given in units of the lattice parameter. The thick bars to the left and right of the ordinate axis present the Mn 3d contribution into the hole for LDA and LDA+U calculations

Table 1. Hole distribution and Mn 3d contribution (in percent). As-1, As-2, N-1 and N-2 denote the first and second coordination spheres of As and N

	(GaMn)As			(GaMn)N		
	Mn(Mn3d)	As-1	As-2	Mn(Mn3d)	N-1	N-2
LDA	29(16)	35	14	50(43)	33	5
LDA+U	9(4)	45	23	25(19)	48	12

interactions with account for the complexity of the electron structure of the systems is necessary.

Another important conclusion from the analysis of Fig. 13 and Table 1 concerns the influence of the Hubbard U on the hole localization and the p–d interaction. For both systems, the account for the on-site Coulomb interaction beyond the LDA leads to a strongly increased hole delocalization and, simultaneously, to decreased p–d interaction. In (GaMn)As, the Mn 3d contribution to the hole drops from 16% to a small value of 4%. For (GaMn)N we get 43% and 19% and the p–d interaction is still strong. Again the resulting influence of U on the Curie temperature cannot be predicted without direct calculation.

In Fig. 14, we present the calculated Curie temperature as a function of the band occupation, n, for one Mn concentration. It is useful to present the Curie temperature in the form $T_C(n) = (T_C(n) - T_C(1)) + T_C(1)$ where $(T_C(n) - T_C(1))$ gives the hole contribution to the Curie temperature and $T_C(1)$ corresponds to the completely occupied bands and can be treated as

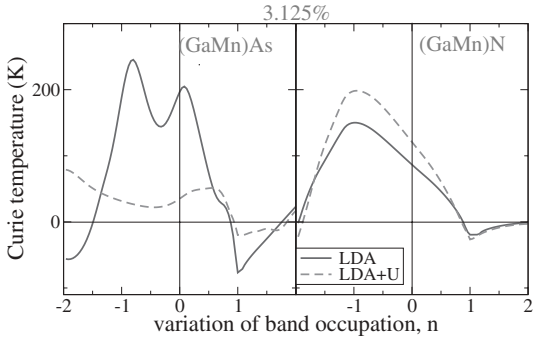

Fig. 14. T_C as a function of the electron number for $x = 3.125\%$. $n = 0$ corresponds to the nominal electron number (one hole per Mn atom)

the contribution of the Anderson's superexchange. Both contributions play an important role (Fig. 14). Thus the final value of the Curie temperature can be interpreted as a result of the competition between antiferromagnetic superexchange through the filled bands and ferromagnetic kinetic exchange mediated by the holes.

It is remarkable that Hubbard U produces opposite trends in the variation of T_C in (GaMn)As and (GaMn)N (Fig. 14). Taking the nominal number of electrons ($n = 0$) we get a strong decrease of the Curie temperature in (GaMn)As and a substantial increase in (GaMn)N. Therefore in (GaMn)As the strong drop of the p–d interaction prevails over the delocalization of the holes. On the other hand, in (GaMn)N the increased delocalization of the holes prevails over decreased p–d interaction.

The comparison of the role of U for different Mn concentrations (Fig. 15) shows that in (GaMn)N the same trend to increasing Curie temperature is obtained for the whole interval of concentrations studied. In (GaMn)As

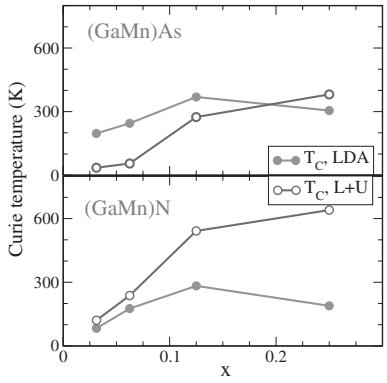

Fig. 15. T_C as a function of the Mn concentration for nominal electron number

there is strong decrease of T_C for low Mn concentrations. For larger x there is a crossover to increasing Curie temperature. These results are in good agreement with the coherent-potential-approximation (CPA) calculations [30] for both systems.

The calculations have demonstrated the importance of both strong p–d interaction and the hole delocalization for the formation of the high-T_C ferromagnetism. These conclusions are in good correlations with a recent model-Hamiltonian study by Bouzerar et al. [31].

8 Conclusions

We have reported density-functional-theory calculations of the exchange interactions and Curie temperature for a series of III-V and II-VI diluted magnetic semiconductors. We focus the discussion on the role of the holes in establishing the ferromagnetic order in various systems. We suggest a method of the quantitative characterization of the properties of the holes. It is shown that there are two conflicting properties of the holes – delocalization from impurity and p–d interaction – whose combination determines the hole influence on the Curie temperature. We demonstrate that Hubbard U increases delocalization of the holes and decreases the strength of p-d interaction. Depending on the system these competing trends can lead to both increase and decrease of the Curie temperature. We show that high value of the Curie temperature for low impurity concentration is possible only in the case of substantial admixture of the impurity 3d states to hole states.

Acknowledgements

The support from Bundesministerium für Bildung und Forschung is acknowledged.

References

1. H. Ohno, A. Shen, F. Matsukura, A. Oiwa, A. Endo, S. Kutsumoto, Y. Iye: Appl. Phys. Lett. **69**, 363 (1996) 113
2. T. Dietl, H. Ohno, F. Matsukura, J. Cibert, D. Ferrand: Science **287**, 1019 (2000) 113
3. N. Theodoropoulou, A.F. Hebard, M.E. Overberg, C.R. Abernathy, S.J. Pearton, S.N.G. Chu, R.G. Wilson: Appl. Phys. Lett. **78** 3475 (2001) 113
4. M.L. Reed, N.A. El-Masry, H.H. Stadelmaier, M.K. Ritums, M.J. Reed, C.A. Parker, J.C. Roberts, S.M. Bedair: Appl. Phys. Lett. **79**, 3473 (2001) 113
5. S. Sonoda, S. Shimizu, T. Sasaki, Y. Yamamoto, H. Hori: J. Cryst. Growth **237**, 1358 ((2002) 113

6. K. Ando: Appl. Phys. Lett. **82**, 100 (2003) 114
7. R. Giraud, S. Kuroda, S. Marcet, E. Bellet-Amalric, X. Biquard, B. Barbara, D. Fruchart, D. Ferrand, J. Cibert, H. Mariette: cond-mat/0307395 114
8. P. Kacman: Semicond. Sci. Technol. **16**, R25 (2001) 114, 124
9. T. Dietl: Semicond. Sci. Technol. **17**, 377 (2002) 114
10. J. König, J. Schliemann, T. Jungwirth, A.H. MacDonald: cond-mat/0111314. 114
11. K. Sato, and H. Katayama-Yosida: Semicond. Sci. Technol. **17**, 367 (2002) 114
12. S. Sanvito, G.J. Theurich, N.A. Hill: J. Superconductivity 15, 85 (2002) 114
13. L.M. Sandratskii, P. Bruno: Phys. Rev. B **66**, 134435 (2002) 114, 115
14. L.M. Sandratskii, P. Bruno: Phys. Rev. B **67**, 214402 (2003) 114, 115, 117
15. G. Bouzerar, J. Kudrnovský, L. Bergqvist, P. Bruno: Phys. Rev. B **68**, 081203 (2003) 114
16. L. Bergqvist, P.A. Korzhavyi, B. Sanyal, S. Mirbt, I.A. Abrikosov, L. Nordström, E.A. Smirnova, P. Mohn, P. Svedlindh, O. Eriksson: Phys. Rev. B **67**, 205201 (2003) 114
17. K. Sato, P.H. Dederics, H. Katayama-Yoshida: Europhys. Lett. **61** 403 (2003) 114
18. In the nonrelativistic systems with collinear magnetic structure the exchange interaction takes place between the states with the same spin projection. 114
19. V.I. Anisimov, F. Aryasetiawan, A.I. Lichtenstein: J. Phys.: Condens. Matter **9**, 767 (1997) 115
20. L.M. Sandratskii: Phys. Rev. B **68**, 224432 (2003) 115, 130
21. L.M. Sandratskii: Advances in Physics **47**, 91 (1998) 115
22. J. Okabayashi, A. Kimura, O. Rader, T. Mizokawa, A. Fujimori, T. Hayashi, M. Tanaka: Phys. Rev. B **58**, 4211 (1998) 116, 123
23. K.C. Ku, S.J. Potashnik, R.F. Wang, S.H. Chun, P. Schiffer, N. Samarth, M.J. Seong, A. Mascarenhas, E. Johnston-Halperin, R.C. Myers, A.C. Gossard, D.D. Awschalom: Appl. Phys. Lett. **82**, 2302 (2003) 119
24. F. Matsukura, H. Ohno, A. Shen, Y. Sugawara: Phys. Rev. B **57**, 2037 (1998) 120, 123
25. H. Saito, V. Zayets, S. Yanagata, K. Ando: Phys. Rev. Lett. **90** 207202 (2003) 121
26. L.M. Sandratskii, P. Bruno: J. Phys.: Cond. Matt. **15**, L585 (2003) 121
27. J.K. Furdyna: J. Appl. Phys. **64**, R29 (1988) 123
28. J. Szczytko, W. Mac, A. Stachow, A. Twardowski, P. Becla, J. Tworzydlo: Solid State Commun. **99**, 927 (1996) 123
29. (ZnMn)Se is not ferromagnetic. Instead for low Mn concentration it shows an interesting combination of giant Zeeman splitting with the absence of any magnetic ordering up to very low temperatures. The reader is referred to [20] for detailed discussion of this system. 125
30. L.M. Sandratskii, P. Bruno, J. Kudrnovský: Phys. Rev. B **69** (2004) 125, 129
31. G. Bouzerar, J. Kudrnovský, P. Bruno: Phys. Rev. B **68**, 205311 (2003) 129